ARTICLE INFO
Article ID: 08-07-02-0010

doi:10.4271/08-07-02-0010

Combined Battery Design Optimization and Energy Management of a Series Hybrid Military Truck

Zifan Liu and Abdullah-Al Mamun Mamun, *Clemson University, USA*
Denise M. Rizzo, *U.S. Army TARDEC, USA*
Simona Onori, *Stanford University, USA*

Abstract

This article investigates the fuel savings potential of a series hybrid military truck using a simultaneous battery pack design and powertrain supervisory control optimization algorithm. The design optimization refers to the sizing of the lithium-ion battery pack in the hybrid configuration. The powertrain supervisory control optimization determines the most efficient way to split the power demand between the battery pack and the engine. Despite the available design and control optimization techniques, a generalized mathematical formulation and solution approach for combined design and control optimization is still missing in the literature. This article intends to fill that void by proposing a unified framework to simultaneously optimize both the battery pack size and power split control sequence. This is achieved through a combination of genetic algorithm (GA) and Pontryagin's minimum principle (PMP) where the design parameters are integrated into the Hamiltonian function. As GA and PMP are global optimization methodologies under suitable conditions, the solution can be considered as a benchmark for the application under study. Five military drive cycles are used to evaluate the proposed approach. The simulation results show 5%-19% reduction in fuel consumption depending on the drive cycle compared to a baseline non-optimized case.

History

Received: 28 Mar 2018
Revised: 20 May 2018
Accepted: 29 Jun 2018
e-Available: 31 Oct 2018

Keywords

HEVs, optimization, Genetic Algorithm, military hybrid vehicles, Pontryagin's Minimum principle

Citation

Liu, Z., Mamun, A., Rizzo, D., and Onori, S., "Combined Battery Design Optimization and Energy Management of a Series Hybrid Military Truck," *SAE Int. J. Alt. Power.* 7(2):2018, doi:10.4271/08-07-02-0010.

ISSN: 2167-4191
e-ISSN: 2167-4205

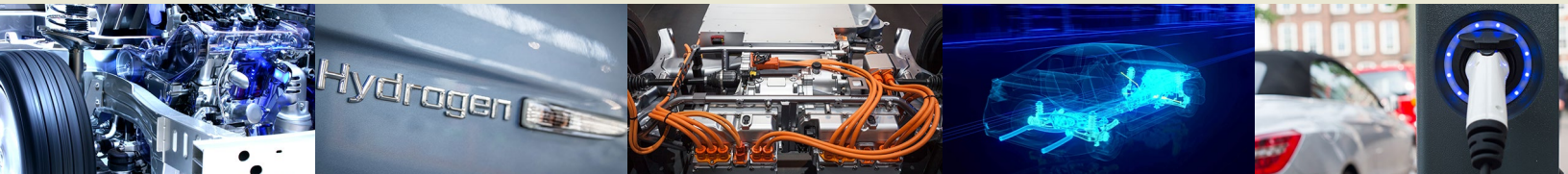

Introduction

Military vehicles require increased power and energy for superior dynamic performance, reliable power exportability, and durable silent watch capability when compared to passenger vehicles. Yet enhancing the fuel efficiency of military vehicles is an important issue that needs to be addressed [1]. Hybridization of the military vehicle powertrain is seen as a potential mean to achieve significant fuel efficiency improvement while providing the required performance. Hybrid electric vehicles (HEVs) combine multiple power sources to enable fuel-saving functions, such as regenerative braking, engine idling elimination, and efficient engine operating region shift. However, the deployment of military HEVs is still under active research due to challenges such as reliability in complex operating and environmental conditions [2]. The focus of this article is to develop a systematic approach to optimize the design and energy management of military HEVs, accounting for specific military driving conditions.

In HEVs, a high-level supervisory energy management strategy (EMS) manages the energy flow among different power sources at each time instant. The objective of the EMS is to achieve certain tasks, such as minimization of fuel consumption and/or tailpipe emission and/or battery health degradation, under appropriate constraints, satisfactory drivability, and component specifications [3]. The highest benefits out of powertrain hybridization are achieved under the optimal component design and optimal power split between the engine and the energy storage system (ESS).

Different optimization algorithms have been proposed in the literature for the design optimization and energy management for HEV application. The design space of an HEV powertrain is nonlinear and often discontinuous due to the complex interconnection among mechanical, electrical, and thermodynamic devices [4]. For HEV design optimization, gradient-free algorithms are more suitable than gradient-based algorithms since they explore the entire design space for the global solution [5, 6]. Some of the popular candidates for gradient-free algorithms are Dividing Rectangles (DIRECT), simulated annealing (SA), genetic algorithm (GA), particle swarm optimization (PSO), etc. [6].

EMSs for HEVs can be generally classified into optimal and suboptimal strategies. Optimal EMSs are obtained by minimizing one or more objectives for off-line benchmarking for a given drive cycle. In a real-time setting, only suboptimal EMSs can be implemented since future driving conditions are unknown. In the category of optimal off-line strategies, dynamic programming (DP), based on Bellman's principle of optimality, guarantees the global optimal solution by searching through all possible power trajectories [7]. The Pontryagin's minimum principle (PMP) is a general case of the Euler-Lagrange equation in the calculus of variation and provides necessary conditions of optimality [8]. Equivalent consumption minimization strategy (ECMS) also produces off-line benchmarking solution where an equivalent fuel consumption is associated with the use of electrical energy from the ESS. The equivalence factor in ECMS is similar to the co-state of PMP which determines the power split based on the instantaneous cost of a virtual equivalent fuel consumption. The analytical formulation of the equivalent fuel consumption in ECMS can be derived using PMP and guarantees the necessary condition of optimality given the a priori information of the drive cycle [9]. Suboptimal strategies are energy management power split laws that are used for online implementation. Rule-based strategies are developed based on heuristics [10, 11, 12] or from DP [13] and do not require any prior knowledge of the drive cycle. Real-time implementation of PMP (or ECMS), possible upon real-time adaptation of the co-state (or equivalence factors) from battery state of charge (SOC) feedback, is known as adaptive ECMS (A-ECMS) [14]. Other strategies such as model predictive control (MPC) [15, 16, 17] or optimal nonlinear regulation strategy which guarantee stability have also been proposed in the literature [18]. Despite the wealth of solutions proposed for energy management and design optimization problem, there have been no unified or integrated approaches proposed to resolve a combined design and control optimization problem. To address this issue, a systematic framework has been proposed in this article to optimize both the design and energy management in military HEVs.

In [19], the strategies to combine both design and control optimization for HEVs have been grouped into sequential, iterative, and simultaneous ones. Both the sequential [20] and iterative [21] strategies decouple the HEV design and control optimization problem. Iterative strategies optimize the plant with the fixed controller and then optimize the controller with the fixed plant, and the process is repeated until convergence is reached. The sequential design and control optimization includes bi-level or two layer methods where the controller is fully optimized for each candidate design. The simultaneous strategies, which vary the design and control parameters at the same time, have also been discussed widely. In [22, 23, 24], GA and a rule-based EMS were integrated for simultaneous optimization. The authors of [4] studied the cooperation of PSO and rule-based EMS. The drawbacks of such an optimization are the inherent suboptimality of the solution and the introduction of many tuning parameters. GA and PSO have also been combined with DP for optimal sizing and control strategies for HEV in a layered fashion [25, 26]. The computational intensity of DP accelerates sharply as the number of design and control parameters increases. Recently, convex programming (CP) has been adopted in [19, 27] for simultaneous design and control optimization; yet the model requires a large number of simplifications to be expressed into a convex form. A similar approach in [28] combines GA and ECMS, where a very large design and control parameter space is evaluated.

This article proposes the novel integration of GA and PMP for the simultaneous design and control optimization of a military hybrid electric truck. A detailed mathematical formulation of combined optimization problem is presented

in this work. The design variables of the battery pack and control variable of the energy management are optimized in the GA routine for global minimum fuel consumption. An electrothermal battery model, the parameters of which have been identified using data from experimental testing on SONY US18650VTC4 Nickel-Manganese-Cobalt-Oxide (NMC) lithium-ion cells, has been utilized in the studies undertaken. Different military drive cycles are used in this study for the evaluation of the impacts of real-world military driving conditions [40].

In the following sections, the notional Mine-Resistant Ambush-Protected All-Terrain Vehicle (M-ATV) model, its components, and the a new experimentally validated battery model are reviewed. The mathematical formulation of the optimization problem is presented and a new solution procedure through GA and PMP and their integration is elaborated. The results of simultaneous optimization of the battery pack design and the control variables are reported for different military drive cycles. Finally, conclusions and lessons learned from the study are presented.

Vehicle Model Description

This study focuses on the powertrain design and energy management of a notional M-ATV [29]. A series hybrid powertrain model of the vehicle is obtained from [30], and the vehicle specifications are summarized in Table 1. The feedforward fuel control path in the vehicle simulator is removed to reduce the number of tuning parameters. The performance of the HEV simulator in terms of fuel consumption without the feedforward fuel control is considered as the baseline against which the solution of the proposed optimization algorithm is compared. It must be noted that the proposed optimization algorithm is based on a vehicle simulator which does not utilize any feedforward fuel control, to ensure an unbiased comparison against the baseline. The series hybrid electric vehicle (SHEV) configuration comprise of a genset (Navistar 6.4L 260 kW diesel engine + 265 kW generator), four 95 kW brushless permanent magnet direct current (BLPMDC) motors, and a 9.6 kWh battery pack with lithium-iron-phosphate (LFP) cells. Figure 1(a) shows a schematic of the hybrid configuration and power flow among different components. A forward-looking simulator is set up in Simulink to model the power flow in which a virtual "driver" in the form of PID controller takes in the speed trace following error to calculate the demanded propulsion power (P_{req}). The genset and the motor are represented by their quasi-static efficiency maps. A supervisory controller based on frequency domain power distribution (FDPD) strategy is implemented for energy management [30].

TABLE 1 Vehicle powertrain and energy storage specifications.

Parameter	Unit	Value
Vehicle		
Total weight	kg	14,023
Frontal area	m^2	5.72
Aerodynamic drag coefficient		0.7
Rolling resistance coefficient		0.01
Tire radius	m	0.59
Genset + Motor		
Engine power	kW	260
Generator power	kW	265
Motor power	kW	4x95=380
Motor rated voltage	V	430
Battery Cell		
26650 Lithium-iron-phosphate (LFP)		
Cell nominal capacity	Ah	2.3
Cell nominal voltage	V	3.3
Cell discharge current/voltage limit	A/V	60/2.5
Cell charge current/voltage limit	A/V	10/4.2
18650 Lithium-ion Nickle-Manganese-Cobalt (NMC)		
Cell nominal capacity, Q_{nom}	Ah	2
Cell nominal voltage	V	3.7
Cell discharge current/voltage limit	A/V	30/2.5
Cell charge current/voltage limit	A/V	12/4.2

FIGURE 1 (a) Representation of the powertrain configuration of a series HEV military truck (adapted from [39]). (b) Block diagram representing the components of the modified forward-looking vehicle simulator.

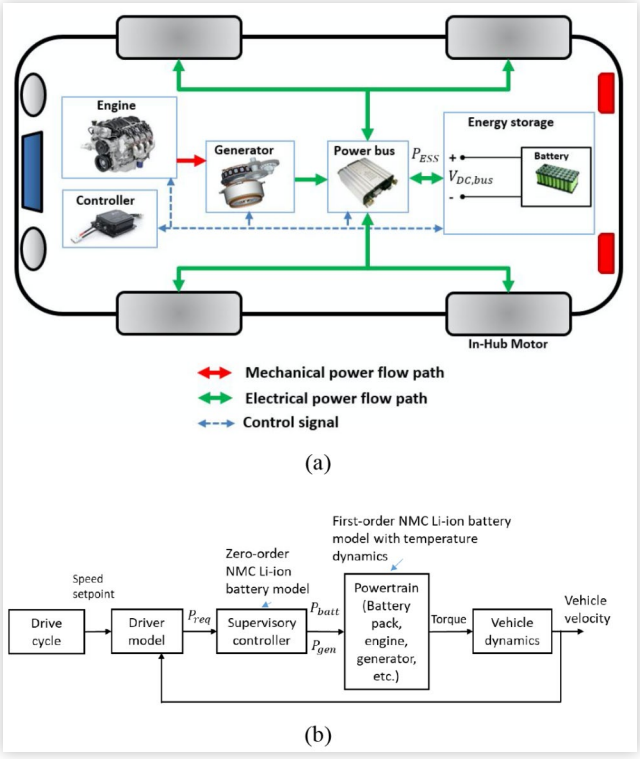

A number of modifications are made to the baseline vehicle simulator before using it for combined design optimization and energy management. A block diagram of the modified forward-looking simulator is shown in Figure 1(b). The LFP battery model is replaced with an NMC battery model. The NMC battery pack in the vehicle simulator is modeled by a first-order equivalent circuit model (ECM) including temperature dynamics. The supervisory controller modified for this work, however, has a zero-order ECM which is used for making the power split decision (Figure 1(b)). The supervisory controller splits the required propulsion power $P_{req}(t)$ into power demanded from the battery pack $P_{batt}(t)$ and the genset $P_{gen}(t)$. The NMC cell model parameters are identified and the model is validated using experimental data collected at the Battery Aging and Characterization (BACh) Laboratory at the Department of Automotive Engineering, Clemson University. The dynamic cell behavior is captured using a first-order ECM as shown in Figure 2. The series resistance R_o represents the internal resistance of the cell, and the resistance-capacitance (RC) pair represents the slow diffusion dynamics of the cell. The resistance and capacitance of the RC pair are defined as R_1 and C_1, respectively. The ECM has two state variables, SOC and the voltage across the capacitor, V_c. The state equations describing the dynamic behavior of the NMC cell are provided in Equations 1 and 2 and the cell voltage equation is given in Equation 3. The nominal cell parameters are obtained from the manufacturer specifications and presented in Table 1. To identify the parameters of the ECM, capacity test and hybrid pulse power characterization (HPPC) tests are performed. The open circuit voltage E_0 is measured from C/20 low current rate discharge capacity test at 23°C and 45°C. The electrical parameters R_o, R_1, and C_1 are identified using the PSO algorithm for discharge and charge scenarios under temperatures of 23°C and 45°C and SOC from 20% to 90% as shown in Figure 4. During simulation, the values of R_o, R_1, and C_1 corresponding to a certain SOC, core temperature (T_c), and current directionality are obtained through interpolation based on the identified values of R_o, R_1, and C_1. Figure 3 illustrates the results of parameter identification studies from HPPC tests conducted at 23°C and 45°C. The figure shows that the root-mean-square (RMS) errors between the measured and simulated cell voltage under 23°C

FIGURE 2 Schematic representation of a first-order ECM. E_o is obtained using C/20 capacity test in discharge experiments, while R_o, R_1, and C_1 are obtained from parameter identification using experimental data from HPPC test.

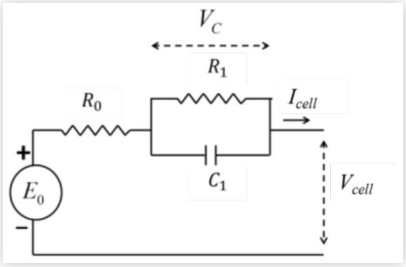

FIGURE 3 Parameter identification results, with the input current shown in the top plot. The comparison of the cell voltage responses between the ECM and the experimental data under the HPPC test is shown for 23°C (middle plot) and 45°C (bottom plot).

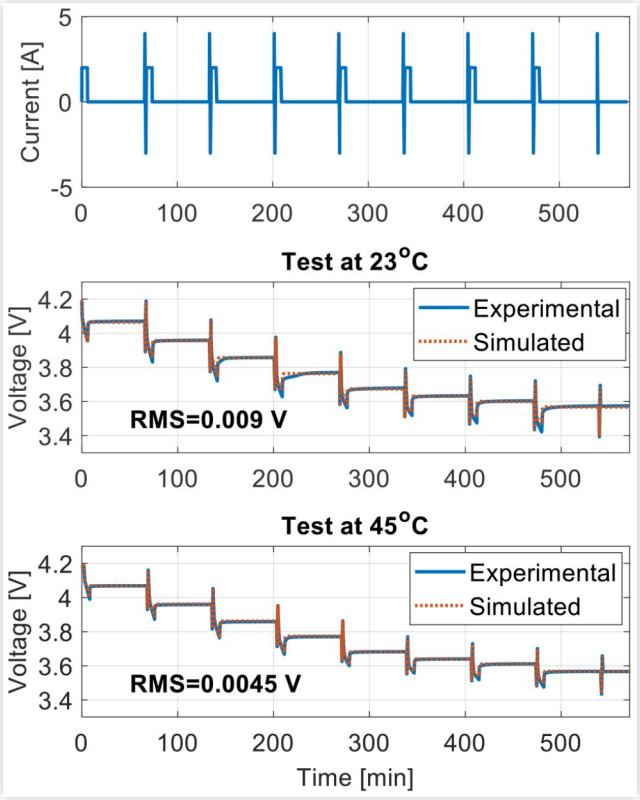

FIGURE 4 Variation of the identified ECM model parameters (R_o, R_1, C_1) based on surface temperature, SOC, and current directionality (charge/discharge).

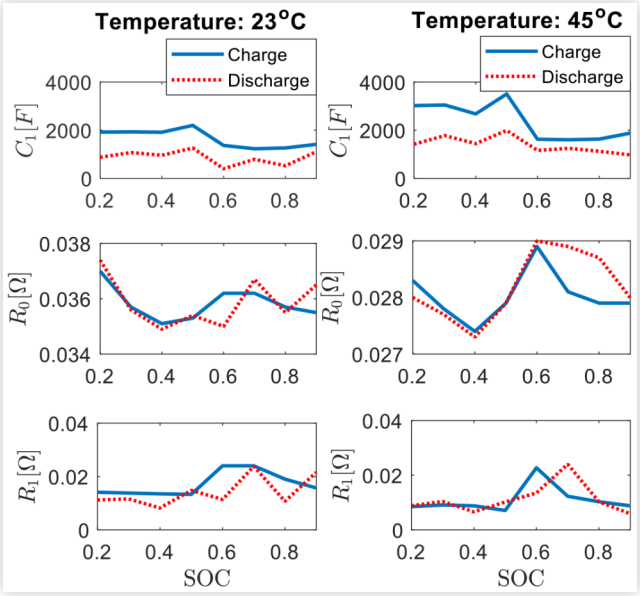

FIGURE 5 (Top) Input current profile of the US06 (×4) cycle obtained from [31]. (Bottom) Comparison between the experimental cell voltage [31] and simulated cell voltage from the identified ECM shows that the model captures the voltage response with an RMS of 8.3 mV.

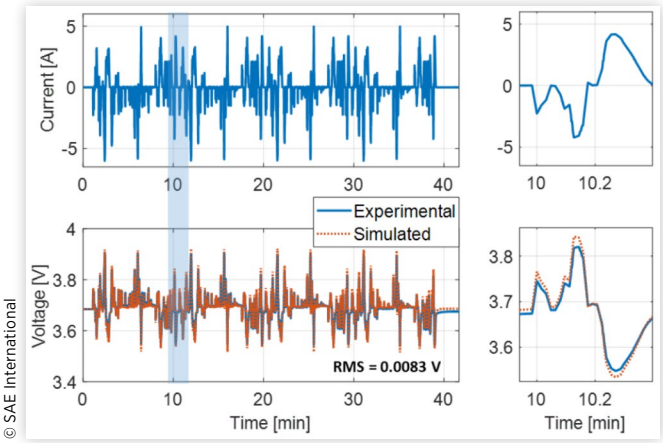

and 45°C are 9 mV and 4.5 mV, respectively. Figure 5 shows the validation results of the identified ECM model using a US06 (x4) drive cycle obtained from [31]. The RMS error obtained from the model validation is 8.3 mV.

$$\dot{V}_c(t) = -\frac{V_c(t)}{R_1(SOC,T_c)\cdot C_1(SOC,T_c)} + \frac{I_{cell}(t)}{C_1(SOC,T_c)} \quad \text{Eq. (1)}$$

$$\dot{SOC}(t) = -\frac{I_{cell}(t)}{3600\cdot Q_{nom}} \quad \text{Eq. (2)}$$

$$V_{cell} = E_0(SOC,T_c) - R_0(SOC,T_c)I_{cell}(t) - V_c(t) \quad \text{Eq. (3)}$$

A two-state temperature model is designed to predict the thermal behavior of the NMC lithium-ion cell [32]. The model has two state variables: the cell surface temperature, T_s, and the core temperature, T_c, as shown in Figure 6. The state

FIGURE 6 Schematic of a two-state thermal model for a lithium-ion battery where surface temperature T_s and core temperature T_c are the state variables [32].

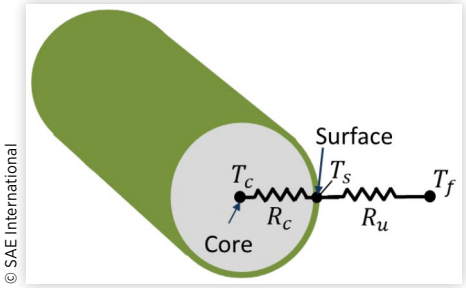

FIGURE 7 For the input current in the top plot, the cell surface temperature (middle plot) and cell core temperature (bottom plot) are measured and used to fit the thermal model. Calculated RMS errors show that the thermal model captures the measured core and surface temperature dynamics within an RMS error of 0.58°C and 0.45°C, respectively. The experiment was conducted with the surrounding temperature at 22.2°C.

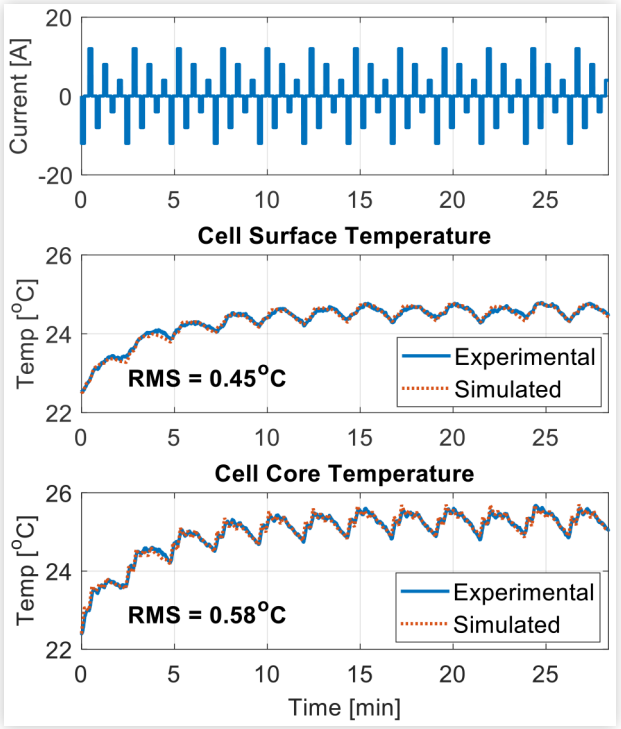

equations are obtained through energy balance and summarized in Equation 4 and 5. The heat generation rate due to chemical reaction, $\dot{Q}$, is defined in Equation 6 using electrical circuit parameters. To identify the thermal model parameters, a customized current profile shown in Figure 7 is used. The surface temperature T_s and the core temperature T_c are measured using thermocouples, and from the measurement, the heat conduction resistance R_c, the heat convection resistance R_u, the heat capacity of the cell core C_c, and the heat capacity of the cell casing C_c are identified. The comparison between the thermal model response and the experimental data in terms of surface and core temperature shows an RMS of 0.45°C and 0.58°C, respectively:

$$C_c\frac{dT_c}{dt} = \dot{Q} + \frac{T_s - T_c}{R_c} \quad \text{Eq. (4)}$$

$$C_s\frac{dT_s}{dt} = \frac{T_f - T_s}{R_u} - \frac{T_s - T_c}{R_c} \quad \text{Eq. (5)}$$

$$\dot{Q} = (E_0 - V_{cell})\cdot I_{cell} \quad \text{Eq. (6)}$$

Combined Optimal Design and Energy Management Problem

The goal of this article is to develop a unified framework to tackle, simultaneously, the design optimization problem and optimal energy management problem with application to military HEVs.

Traditionally, the optimal component sizing problem and the energy management problem have been solved in a layered fashion. On the outer layer, an exhaustive search or heuristic global search algorithm, such as GA, PSO, etc., is typically employed to randomly select a battery pack size. In the inner layer, an optimal energy management algorithm, such as DP, PMP, rule-based EMS, etc., is used to find the optimal energy split among different energy devices at every time step [25, 26, 28]. In [28], such a layered optimization algorithm is proposed where vehicle architecture parameters, such as the number of the motor per axle, number of axles, size, and type of energy storage, are considered as the design variables. It has six objective functions and fuel consumption minimization found through ECMS is one of them. A similar approach is proposed in [26], where GA is used in the outer loop for battery and supercapacitor sizing and DP is used in the inner loop to find the optimal power split between them. In these approaches, the interaction between the design parameters and control strategy is from top to bottom resulting in a bi-level iterative process. Such processes increase the computational time and complexity, so multiple design variables are visited and evaluated for which the control strategies might not be feasible in the first place. In this article, a combined optimization framework where control variables of the bottom level are optimized simultaneously with the design variables in the top level is proposed. The proposed approach formulates the Hamiltonian function by incorporating both the design and control variables. In this combined approach, the differential evolution (DE) algorithm, which is a GA-based heuristic algorithm, and the PMP are used together. PMP is suitable for such a combined approach because of its structure. Unlike DP algorithm which suffers from the "curse of dimensionality," PMP minimizes a cost function by minimizing the Hamiltonian with less computation even for a large number of state variables. DP uses a backward simulation approach from the end of time in a discrete state space. The optimality of the solution from DP is guaranteed only up to a certain level of discretization [8]. PMP solves the problem forward in time, which makes it possible to use a more complex forward-looking model. The solution of PMP is obtained by solving a two-point boundary value problem. However, in HEV control with a lithium-ion battery pack, the dependency of the co-state dynamics on the SOC is neglected and a constant co-state is assumed [33]. This assumption greatly simplifies the optimization problem formulated using PMP. The next section describes a mathematical formulation of the design and optimal control problem.

Problem Formulation

In this work, the overall objective is to minimize the total vehicle fuel consumption over a given drive cycle over the time horizon $[0, t_f]$:

$$J = \int_0^{t_f} \dot{m}_{fuel}\left(P_{batt}(t)\right)dt \qquad \text{Eq. (7)}$$

where $\dot{m}_{fuel}$ is the fuel mass flow rate (kg/s) which is a function of the instantaneous power demand from the battery pack, $P_{batt}(t)$. Assuming homogeneity in the battery pack, the power delivered from the pack can be expressed as a product of the number of lithium-ion cells in a series string N_s, number of parallel strings N_p, and power delivered by a single cell $P_{cell}(t)$. For the problem formulation, the battery pack SOC is defined as $x(t)$, the power from a cell is defined as $u(t)$, and battery design vector is defined as $\boldsymbol{v}$, where $\boldsymbol{v} = [N_s\ N_p]^T$. The goal of the optimization problem is to find the admissible design and control variables π:

$$\boldsymbol{\pi}(t) = \begin{cases} u(t) \in U(t) \\ \boldsymbol{v} \in \boldsymbol{V} \end{cases} \qquad \text{Eq. (8)}$$

where $U(t) = [u_{min}(t), u_{max}(t)]$ and $\boldsymbol{V} = [\boldsymbol{v_{min}}, \boldsymbol{v_{max}}]$, such that

$$J = \int_0^{t_f} \dot{m}_{fuel}\left(u(t), \boldsymbol{v}\right)dt \qquad \text{Eq. (9)}$$

subject to

$$\begin{aligned}
&\dot{x}(t) = f\left(t, x(t), u(t)\right) \\
&\boldsymbol{v}_{min} \le \boldsymbol{v} \le \boldsymbol{v}_{max} \\
&x\left(t_f\right) - x_{target} = \Delta x = 0 \\
&u_{min}(t) \le u(t) \le u_{max}(t) \\
&x_{min}(t) \le x(t) \le x_{max}(t) \\
&T_{y,min} \le T_y(t) \le T_{y,max} \\
&\omega_{y,min} \le \omega_y(t) \le \omega_{y,max} \\
&y = engine, motor, generator
\end{aligned}$$

where T denotes torque and ω denotes angular speed of the engine, the motor, and the generator.

The PMP has been successfully implemented to solve the optimal power split problem in HEVs [33, 34]. In this formulation, SOC $x(t)$ is the state variable and input power $u(t)$ is the control input. For the given objective, the Hamiltonian function is defined as follows:

$$H\left(t, x(t), u(t), \boldsymbol{v}\right) = \dot{m}_{fuel}\left(u(t), \boldsymbol{v}\right) + \lambda(t) \cdot f\left(t, x(t), u(t)\right) \qquad \text{Eq. (10)}$$

where λ is the co-state in units of kilograms and f represents the state dynamics of the battery pack. The temperature-dependent two-state lithium-ion battery model presented in Equations 1-6 is implemented in the powertrain of the vehicle

simulator. However, for making the power split decision in the supervisory controller, a simpler zero-order ECM of a lithium-ion battery is used to define the battery SOC, $x(t)$ as a function of the control variable. The necessary conditions for optimality of the Hamiltonian are the following:

State dynamics

$$\dot{x}(t)=\frac{\partial H}{\partial \lambda}=-\frac{I_{batt}}{Q_{pack}}=-\frac{I_{cell}}{Q_{nom}}=\frac{E_0-\sqrt{E_0^2-4R_0u(t)}}{2R_0Q_{nom}} \quad \text{Eq. (11)}$$

Co-state dynamics

$$\dot{\lambda}(t)=-\frac{\partial H}{\partial x}=-\lambda\frac{\partial \dot{x}}{\partial x}=-\lambda\frac{\partial}{\partial x}\left(\frac{E_0-\sqrt{E_0^2-4R_0u(t)}}{2R_0Q_{nom}}\right) \quad \text{Eq. (12)}$$

Charge sustainability

$$x(t_f)-x_{target}=\Delta x=0 \quad \text{Eq. (13)}$$

Stationarity

$$\pi^*(t)=\operatorname{argmin}\left(H(t,x(t),\lambda(t),u(t),v)\right)$$
$$u(t)\in U(t) \quad \text{Eq. (14)}$$
$$v\in V$$

Under an HEV charge sustaining operation, the battery SOC is usually constrained within a narrow window. Within that range, E_0 and R_0 can be assumed as constant, and $\dot{x}(t)$ depends only on cell power $u(t)$. Therefore, the co-state dynamics $\dot{\lambda}(t)$ given in Equation 12 becomes zero and $\lambda(t)$ becomes a constant [5].

Solution Method

For a given military drive cycle, the problem formulation described in the previous section is used to find a global solution for minimum fuel consumption. DE is used to solve the fuel consumption minimization problem. It is a variation of GA, where the real encoding of floating point numbers and the nonuniform crossover are used. DE is easier to tune compared to other evolutionary algorithms [35] and it was first proposed in [36]. In this work, a modified version of the DE algorithm, similar to the one in [37], is used and applied to the optimal battery pack design and control problem for the military SHEV. The design variables are the number of lithium-ion cells in series, N_s, and the number of lithium-ion cells in parallel, N_P. The control variable is the power split decision at each time step between the engine and the battery pack. Since the co-state variable λ is a measure of the cost of using electric energy from the battery, the optimal value of λ determines the optimal power split at each time step. Therefore, in the global optimization framework, the decision variables are the number of cells in series N_s, the number of cells in parallel N_p, and the co-state λ. At the initialization phase of the optimization, an initial population of N members is generated, where each population member has a different combination of these three decision variables. Through crossover and mutation, a larger population set is generated. If any population member violates the constraints of the optimization problem, that member is discarded and a new member is generated. To generate a set of candidate solutions, the charge sustaining constraint in Equation 13 is relaxed and a population member is considered feasible if the final SOC is within 0.25% of the initial SOC. For each population member, the Hamiltonian function is minimized at every time step while satisfying the constraints of state and co-state dynamics in Equations 11 and 12. From the optimal battery power corresponding to the minimum value of the Hamiltonian, the total fuel consumption over the drive cycle for each population member is obtained using Equation 9. Based on the fuel consumption of each member, a small set of population members are selected. The process is then repeated in the next generation until the stopping criteria (M number of generations) are achieved. Then the best combination of the decision variables with the minimum fuel consumption is selected. This global solution approach eliminates the need of solving a two-point boundary value problem iteratively [25] to find the optimal co-state. In Figure 8, the basic structure of the solution approach used in this article is presented.

FIGURE 8 Flowchart for solving the combined design optimization and optimal energy management problem using GA and PMP.

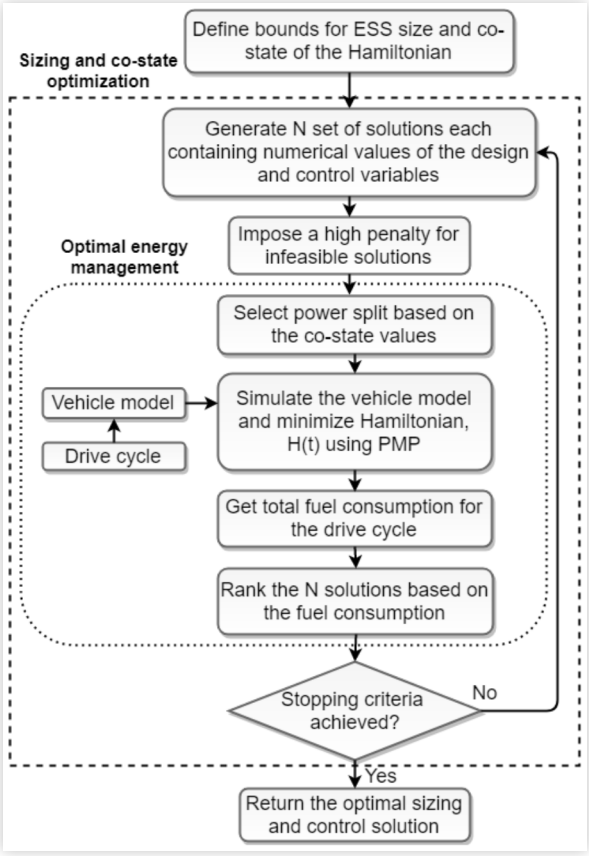

Bounds of Decision Variables

The global optimization algorithm has three decision variables, N_s, N_p, and λ. A design space needs to be specified, within which the optimization algorithm determines the optimal combination of the decision variables. A feasible bound of values for each variable is determined based on the electrical system limitations and vehicle dynamic performance requirements:

1. The bound on N_S is defined by assuming that battery pack voltage, which is equivalent to the DC bus voltage, stays within 90% to 110% of the rated voltage of the DC motor for reliable and safe operation. Thus, N_s must satisfy the inequality constraint in Equation 15. For a DC bus voltage of 429 V, the constraint on the number of cells in series is expressed as

$$V_{DC,BUS} \cdot 90\% \le N_s \cdot V_{Li,nominal} \le V_{DC,BUS} \cdot 110\% \quad \text{Eq. (15)}$$

$$104 \le N_s \le 128 \quad \text{Eq. (16)}$$

2. The energy capacity of the battery pack is assumed to vary within 50% to 110% of the capacity of the original pack on baseline vehicle. This asymmetric inequality constraint, with more emphasis on smaller pack for economic concerns, is illustrated in Equation 17. With nominal cell voltage, V_{cell} = 3.7 V; nominal charge capacity, Q_{nom} = 2 Ah; and energy capacity of the baseline battery pack, $E_{batt,pack}$ = 9867 Wh, the resulting constraint on the number of cells in series and number of parallel strings is given by

$$E_{batt} \cdot 50\% \le N_s \cdot N_p \cdot E_{Li,nominal} \le E_{batt} \cdot 110\% \quad \text{Eq. (17)}$$

$$667 \le N_s \cdot N_p \le 1466 \quad \text{Eq. (18)}$$

3. The value of the optimal co-state λ for military drive cycles is typically around 2.5 for the military HEV with the existing battery pack in this study. So the feasible bound of λ for a search is selected as

$$2 \le \lambda \le 3 \quad \text{Eq. (19)}$$

Results

The simultaneous design and control optimization routine was applied to five military drive cycles: DCE5 Urban Assault, DCE4 convoy Escort, Churchville, Munson, and Harford [38]. Figure 9 shows the performance of the HEV vehicle simulator equipped with the optimal battery pack and PMP-based EMS to follow the desired drive cycle. Cycle following errors

FIGURE 9 Five military drive cycles (blue) are simulated with the optimal battery pack using the proposed combined design and control optimization approach (red dotted line). For all the drive cycles, the simulated vehicle velocity follows the drive cycles, which confirms the validity of the vehicle simulator and the optimal solution.

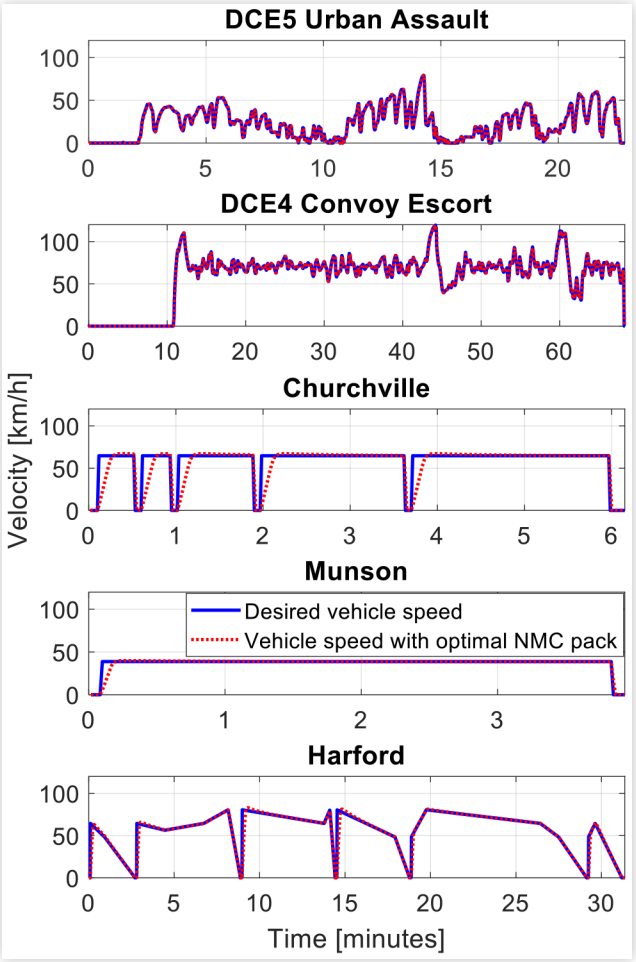

sporadically occur where sharp acceleration power demands are requested, especially in drive cycles such as Churchville and Munson. The value of the optimization variables and the corresponding fuel consumption obtained from the global optimizer for each drive cycle are summarized in Table 2 in the "Optimized NMC Pack" rows. Results obtained from the combined design optimization and energy management are compared against the baseline vehicle simulator with an LFP battery pack [30]. To reduce the number of tuning parameters in the baseline, and to obtain feasible results for all five military cycles, a constant cutoff frequency (0.12 Hz) is used for the frequency-based EMS. The fuel consumption values for the baseline vehicle are listed in the "Baseline with LFP Pack" rows. The results presented in Figure 10 indicate that the proposed approach can reduce the fuel consumption of a series hybrid M-ATV from 4.6% to as high as 19.54% compared to the baseline. In this optimization study, 0.25% difference

TABLE 2 Comparison of the baseline LFP and the optimized NMC battery pack configurations in terms of the number of cells, total weight of the cells, total volume of the cells, co-states, and fuel consumptions for the five military drive cycles. The proposed approach finds the best battery pack configuration and the co-state to minimize fuel consumption within the vehicle design constraints.

	N_s	N_p	Energy capacity (kWh)	Weight (kg)	Volume (m^3)	λ	Fuel consumption (L/100 km)
DCE5 Urban Assault							
Baseline LFP pack	130	10	9.87	98.8	3.45e−3	N/A	**38.06**
Optimized NMC pack	111	13	10.68	66.38	2.71e−3	2.6378	**34.40** (−9.61%)
DCE4 Convoy Escort							
Baseline LFP pack	130	10	9.87	98.8	3.45e-3	N/A	**22.37**
Optimized NMC pack	108	12	9.59	59.62	2.44e-3	2.3235	**21.34** (−4.6%)
Churchville							
Baseline LFP pack	130	10	9.87	98.8	3.45e-3	N/A	**40.1**
Optimized NMC pack	120	09	7.99	49.68	2.03e-3	2.0548	**32.59** (−18.73%)
Munson							
Baseline LFP pack	130	10	9.87	98.8	3.45e-3	N/A	**21.31**
Optimized NMC pack	116	12	10.30	64.03	2.62e-3	2.4009	**17.15** (−19.54%)
Harford							
Baseline LFP pack	130	10	9.87	98.8	3.45e-3	N/A	**21.00**
Optimized NMC pack	119	10	8.81	54.74	2.24e-3	2.0131	**19.01** (−9.49%)

between the initial and final SOC is allowed. Therefore, the optimal solutions for different drive cycles are very close to the charge sustaining case. However, the results from the baseline are often not charge sustaining. For a fair comparison, a correction term is added to the total fuel consumption for the baseline based on the difference between the initial and final SOC of the battery pack outlined in [34].

The fuel consumption reduction compared to the baseline simulator depends largely on the drive cycle characteristics. The DCE4 cycle produces the least amount of fuel consumption reduction, while Munson cycle produces the most amount of reduction. Figure 11 shows the engine operating points, while

FIGURE 10 Comparison of fuel consumption between the baseline vehicle simulator with a fixed LFP battery pack and the PMP-based EMS and vehicle simulator where the NMC battery pack size and power split are optimized through combined design optimization and energy management.

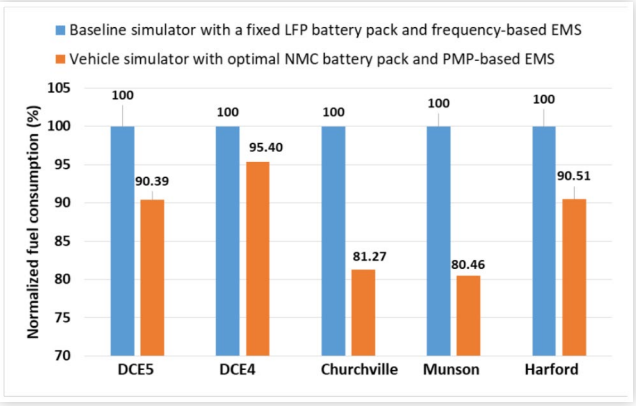

Figure 12 shows the battery SOC and power split between the battery pack and the engine-generator set for DCE4 and Munson cycle. The DCE4 cycle is composed of high-speed driving with frequent speed fluctuations. The optimal control algorithm splits the required power between the engine and the battery pack in such a way that the engine operates close to its optimal operating point compared to the baseline. Due to large fluctuations in the required power, the operating points cannot move very close to the optimal brake-specific fuel consumption (BSFC) point, hence the 4.6% reduction in fuel consumption. The improvement in fuel economy for Munson cycle based on the proposed approach is around 19.54%. Since the drive cycle has a long cruising period, the optimal control algorithm allows the engine operating points to steadily move toward its most efficient zone ("sweet spot"). On the other hand, the baseline simulator splits the power based on the cutoff frequency only and operation close to the efficient zone of the engine is not considered.

Small variation in the baseline vehicle design given in Equations 15 and 17 allows the optimizer to select a battery pack size and control strategy that produces the least amount of fuel consumption for each drive cycle. For two out of five drive cycles, a larger battery pack size in terms of energy capacity is found by the optimizer compared to the original pack in the baseline. It is interesting to note that in three cases, the optimizer yielded battery pack sizes which are smaller than the baseline pack and yet produce better fuel economy. The collective weight and volume of the cells are also computed for better understanding of the optimal solution found for different drive cycles. SOC variation of the battery pack presented in Figure 13 shows that battery use is diminished significantly compared to the baseline strategy. The suppressed battery usage helps push the engine operating points to higher power regions,

FIGURE 11 The engine operating points with the baseline LFP and optimal NMC battery pack along with the engine BSFC contours for DCE4 Convoy Escort (top) and Munson drive cycles (bottom). The reduction in fuel consumption from the baseline vehicle simulator to the optimized vehicle simulator is obtained by shifting the engine operating points toward the more efficient region with a lower average BSFC.

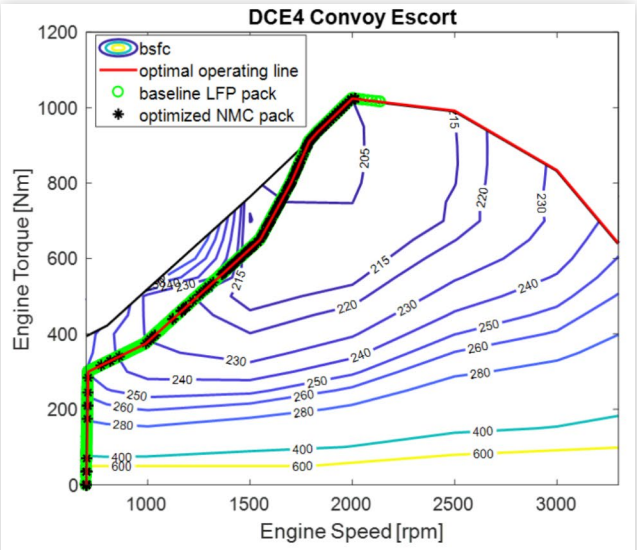

Average BSFC for the baseline LFP pack	149 g/kWh
Average BSFC for the optimized NMC pack	107 g/kWh

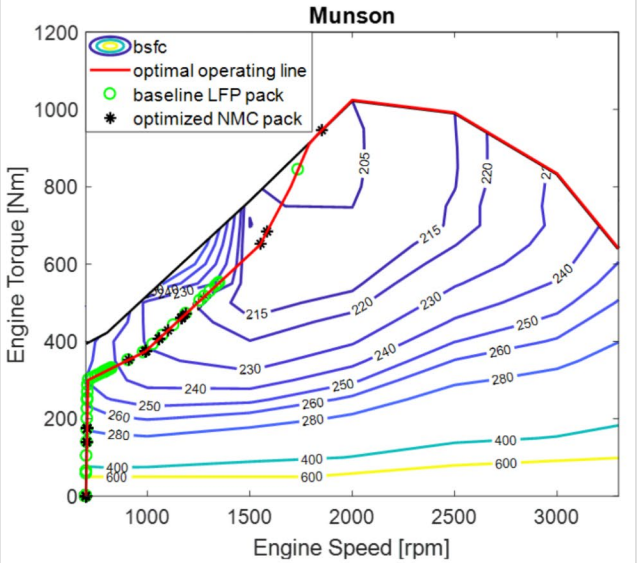

Average BSFC for the baseline LFP pack	177 g/kWh
Average BSFC for the optimized NMC pack	128 g/kWh

FIGURE 12 The power delivered from the battery pack and the engine-generator set for DCE4 Convoy Escort (top) and Munson (bottom) drive cycles using the baseline LFP battery pack and the optimized NMC battery pack.

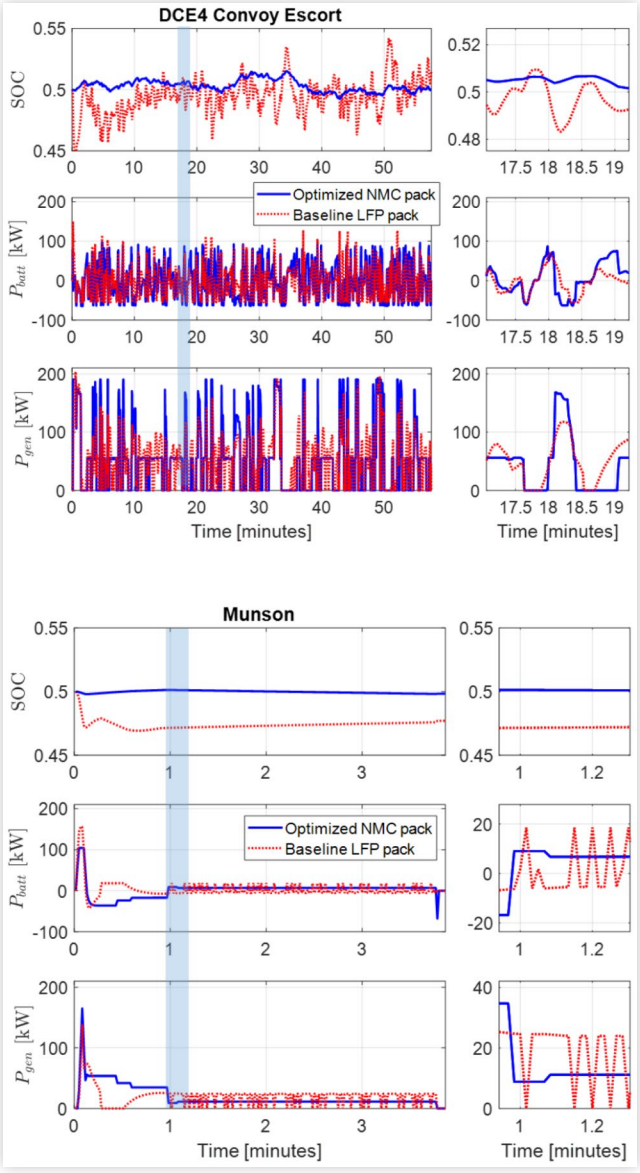

closer to its sweet spot. The small fluctuation in battery SOC also has a potential benefit for long-term battery health.

The results infer that using a single energy storage technology (NMC in this case) and allowing small variations in the total energy storage capacity (50% to 110% of the baseline) yield a 4.6% to 19.54% reduction in fuel consumption, depending on the drive cycle. These results also confirm that the optimization algorithm presented in this article is capable of finding the optimal size of the ESS and power management policy within the allowable design space for minimum fuel consumption. The resulting energy capacity for the NMC battery pack compared to the baseline LFP battery pack is

FIGURE 13 The battery SOC profiles in the baseline LFP battery pack and optimized NMC battery pack configurations for five military drive cycles. The optimal battery pack design and control policy produce less SOC variations compared to the original battery pack across all drive cycles.

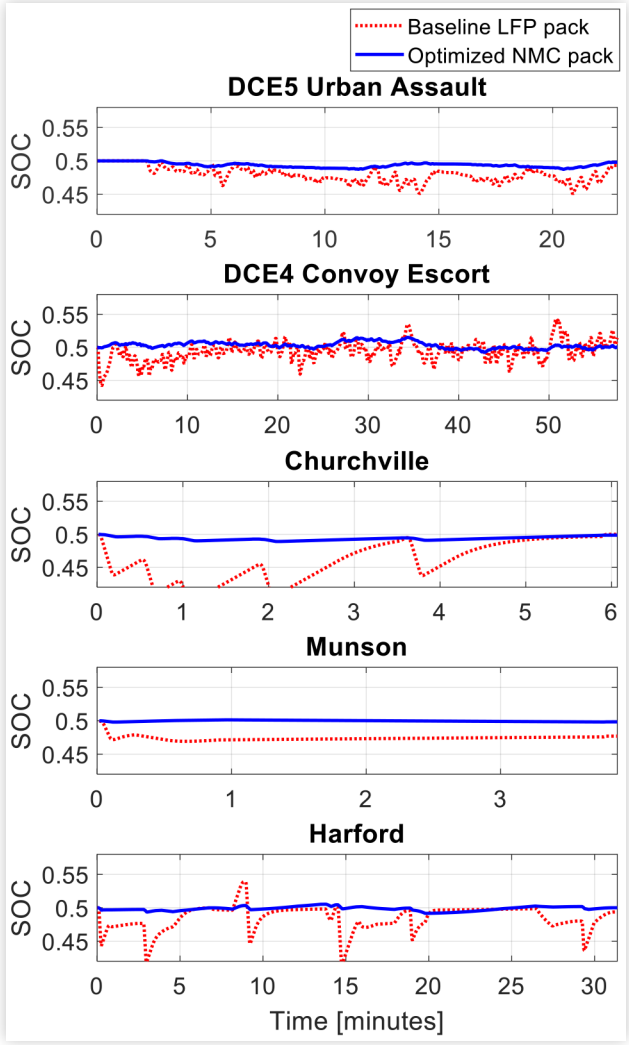

larger for the DCE5 and Munson cycles. For DCE4, Churchville, and Harford drive cycle, lower fuel consumption is obtained using an NMC battery pack with a smaller energy capacity compared to the baseline LFP pack. Therefore, this work shows that based on the drive cycle characteristics, even a smaller battery pack in terms of energy capacity might result in lower fuel consumption. This finding signifies the importance of a combined design optimization and energy management algorithm compared to the control optimization for a fixed design. These results also motivate the inclusion of additional degrees of freedom such as hybrid ESS in the vehicle powertrain to further reduce the fuel consumption. The optimization approach developed in this article is general enough to include additional ESS and powertrain components for better fuel economy or additional objective functions.

FIGURE 14 The acceleration performance test, without grade (top) and with 20% grade (bottom) for the hybrid electric military M-ATV truck using the largest optimized battery pack from Table 2 (N_s = 111, N_p = 13). The truck achieves the 0-60 km/h target in 10.5 seconds (0 km/h at 5 sec and 60 km/h at 15.5 sec) and manages to overcome the 20% grade.

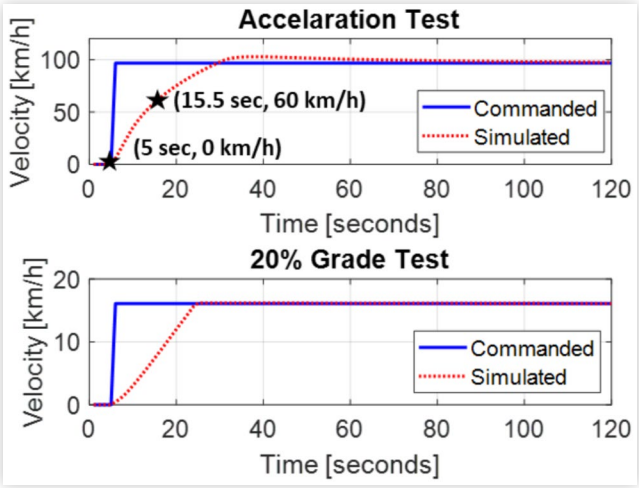

To validate the dynamic capabilities of the hybrid electric military truck, both acceleration and grade tests were performed. The authors of [1] summarize that for a medium-duty truck (gross vehicle weight between 4 and 9 tons), the ability to accelerate from 0 to 60 km/h in less than 22 seconds and traverse at least 20% grade is critical for military applications. These requirements are used to calibrate the dynamic performance of the hybrid electric M-ATV military truck in this study. Figure 14 shows the acceleration and grading performance of the M-ATV SHEV truck with the largest optimized NMC battery pack. The dynamic capability tests were performed under "sport mode" condition, in which both genset and battery are used with their maximum power. With the largest optimized battery pack (N_s = 111, N_p = 13) which is derived for the DCE5 Urban Assault drive cycle, the truck meets the dynamic capability requirements.

Summary

This article proposes a simultaneous design and control optimization routine for a series hybrid military truck. Both the powertrain design and power management strategy are optimized to utilize the maximum benefit from hybridization. The development of such a combined mathematical formulation to find the benchmark design parameters and control solution for HEVs is the novel contribution of this article. The previous literature decoupled the design and control optimization problem by using either sequential or iterative optimization approaches. In this study, the design optimization parameters

are integrated in the Hamiltonian function from PMP. The implementation of the integrated optimization problem uses the co-state λ, the number of battery cells in series and number of battery cells in parallel as decision variables within the GA framework. The hybrid M-ATV military truck with the optimized battery pack can achieve fuel economy benefits spanning from 4.6% to 19.56% across different military drive cycles. Simulation results reveal that SOC variation is smaller than the SOC variation experienced by the battery used in the baseline case. Such a limited variation is beneficial for battery health in the long run. The optimal fuel efficiency obtained in this study cannot be fully achieved in real-time control applications due to the lack of a priori drive cycle information. However, the optimization algorithm proposed provides a benchmark solution that can be used to both evaluate and calibrate online EMSs. For real-time implementation, it is possible to suitably adapt the co-state of the PMP as driving conditions change by means of an adaptive optimal supervisory controller [24]. The simultaneous optimization framework in this study can be generalized to powertrain optimization problem with hybrid ESS as well.

Contact Information

sonori@stanford.edu

Acknowledgment

Unclassified. DISTRIBUTION STATEMENT A. Approved for public release; distribution is unlimited.

This research was supported by the Automotive Research Center (ARC) at the University of Michigan, under Cooperative Agreement W56HZV-14-2-0001 with the U.S. Army Tank Automotive Research, Development, and Engineering Center (TARDEC) in Warren, MI.

Disclaimer: Reference herein to any specific commercial company, product, process, or service by trade name, trademark, manufacturer, or otherwise does not necessarily constitute or imply its endorsement, recommendation, or favoring by the United States Government or the Dept. of the Army (DoA). The opinions of the authors expressed herein do not necessarily state or reflect those of the United States Government or the DoD, and shall not be used for advertising or product endorsement purposes.

References

1. Kramer, D.M. and Parker, G.G., "Current State of Military Hybrid Vehicle Development," *Int. J. Electr. Hybrid Veh.* 3(4):369-387, 2011.
2. Rizzo, D.M., *Military Vehicle Optimization and Control* (Michigan Technological University, 2014).
3. Chan, C.C., "The State of the Art of Electric, Hybrid, and Fuel Cell Vehicles," *Proc. IEEE* 95(4):704-718, 2007.
4. Wu, J., Zhang, C.-H., and Cui, N.-X., "PSO Algorithm-Based Parameter Optimization for HEV Powertrain and its Control Strategy," *Int. J. Automot. Technol.* 9(1):53-59, 2008.
5. Wipke, K., Markel, T., and Nelson, D., "Optimizing Energy Management Strategy and Degree of Hybridization for a Hydrogen Fuel Cell SUV," *Proceedings of 18th Electric Vehicle Symposium*, 2001, 1-12.
6. Gao, W. and Mi, C., "Hybrid Vehicle Design Using Global Optimisation Algorithms," *Int. J. Electr. Hybrid Veh.* 1(1):57-70, 2007.
7. Bertsekas, D.P., *Dynamic Programming and Optimal Control*, Vol. 1, no. 2 (Belmont, MA, Athena Scientific, 1995).
8. Guzzella, L., Sciarretta, A. et al., *Vehicle Propulsion Systems*. Vol. 1 (Springer, 2007).
9. Serrao, L., Onori, S., and Rizzoni, G., "ECMS as a Realization of Pontryagin's Minimum Principle for HEV Control," *American Control Conference, 2009. ACC'09*, 2009, 3964-3969.
10. Salmasi, F.R., "Control Strategies for Hybrid Electric Vehicles: Evolution, Classification, Comparison, and Future Trends," *IEEE Trans. Veh. Technol.* 56(5):2393-2404, 2007.
11. Jalil, N., Kheir, N.A., and Salman, M., "A Rule-Based Energy Management Strategy for a Series Hybrid Vehicle," *American Control Conference, 1997. Proceedings of the 1997*, 1997, Vol. 1, 689-693.
12. Lin, C.-C., Peng, H., Grizzle, J.W., and Kang, J.-M., "Power Management Strategy for a Parallel Hybrid Electric Truck," *IEEE Trans. Control Syst. Technol.* 11(6):839-849, 2003.
13. Bianchi, D. et al., "Layered Control Strategies for Hybrid Electric Vehicles Based on Optimal Control," *Int. J. Electr. Hybrid Veh.* 3(2):191-217, 2011.
14. Onori, S. and Serrao, L., "On Adaptive-ECMS Strategies for Hybrid Electric Vehicles," *Proceedings of the International Scientific Conference on Hybrid and Electric Vehicles*, Malmaison, France, 2011, 6-7.
15. Borhan, H., Vahidi, A., Phillips, A.M., Kuang, M.L. et al., "MPC-Based Energy Management of a Power-Split Hybrid Electric Vehicle," *IEEE Trans. Control Syst. Technol.* 20(3):593-603, 2012.
16. Sampathnarayanan, B., Serrao, L., Onori, S., Rizzoni, G. et al., "Model Predictive Control as an Energy Management Strategy for Hybrid Electric Vehicles," *ASME 2009 Dynamic Systems and Control Conference*, 2009, 249-256.
17. Huang, Y., Wang, H., Khajepour, A., He, H. et al., "Model Predictive Control Power Management Strategies for HEVs: A Review," *J. Power Sources* 341:91-106, 2017.
18. Sampathnarayanan, B., Onori, S., and Yurkovich, S., "An Optimal Regulation Strategy with Disturbance Rejection for Energy Management of Hybrid Electric Vehicles," *Automatica* 50(1):128-140, 2014.
19. Murgovski, N., Hu, X., Johannesson, L., and Egardt, B., "Combined Design and Control Optimization of Hybrid Vehicles," *Handbook of Clean Energy System*, 2014.
20. Panday, A. and Bansal, H.O., "Energy Management Strategy Implementation for Hybrid Electric Vehicles Using Genetic Algorithm Tuned Pontryagin's Minimum Principle Controller," 2016.

21. Filipi, Z. et al., "Combined Optimisation of Design and Power Management of the Hydraulic Hybrid Propulsion System for the 6x6 Medium Truck," *Int. J. Heavy Veh. Syst.* 11(3-4):372-402, 2004.
22. Fang, L.-C. and Qin, S.-Y., "Concurrent Optimization for Parameters of Powertrain and Control System of Hybrid Electric Vehicle Based on Multi-Objective Genetic Algorithms," *SICE-ICASE, 2006. International Joint Conference*, 2006, 2424-2429.
23. Zhang, B. and Chen, Z., "Multi-Objective Parameter Optimization of a Series Hybrid Electric Vehicle Using Evolutionary Algorithms," *Veh. Power* 921-925, 2009.
24. Wu, L., Wang, Y., Yuan, X., and Chen, Z., "Multiobjective Optimization of HEV Fuel Economy and Emissions Using the Self-Adaptive Differential Evolution Algorithm," *IEEE Trans. Veh. Technol.* 60(6):2458-2470, 2011.
25. Nüesch, T., Ott, T., Ebbesen, S., and Guzzella, L., "Cost and Fuel-Optimal Selection of HEV Topologies Using Particle Swarm Optimization and Dynamic Programming," *Proceedings of the 2012 American Control Conference*, 2012, Vol. 1, 1302-1307.
26. Ravey, A., Roche, R., Blunier, B., and Miraoui, A., "Combined Optimal Sizing and Energy Management of Hybrid Electric Vehicles," *Transportation Electrification Conference and Expo (ITEC), 2012 IEEE*, 2012, 1-6.
27. Hu, X., Moura, S.J., Murgovski, N., Egardt, B. et al., "Integrated Optimization of Battery Sizing, Charging, and Power Management in Plug-in Hybrid Electric Vehicles," *IEEE Trans. Control Syst. Technol.* 24(3):1036-1043, 2016.
28. Donateo, T., Serrao, L., and Rizzoni, G., "A Two-Step Optimisation Method for the Preliminary Design of a Hybrid Electric Vehicle," *Int. J. Electr. Hybrid Veh.* 1(2):142-165, 2008.
29. Oshkosh Defense, "Multi-Mission Family of Vehicles M-ATV," 2016, https://oshkoshdefense.com/wp-content/uploads/2016/05/Global-M-ATV-Brochure-5-3-2106.pdf.
30. Kim, Y., Salvi, A., Siegel, J.B., Filipi, Z.S. et al., "Hardware-in-the-Loop Validation of a Power Management Strategy for Hybrid Powertrains," *Control Eng. Pract.* 29:277-286, 2014.
31. Allam, A. and Onori, S., "An Interconnected Observer for Concurrent Estimation of Bulk and Surface Concentration in Cathode and Anode of a Lithium-Ion Battery," *IEEE Trans. Ind. Electron.*, 2018.
32. Lin, X. et al., "A Lumped-Parameter Electro-Thermal Model for Cylindrical Batteries," *J. Power Sources* 257:1-11, 2014.
33. Kim, N., Cha, S., and Peng, H., "Optimal Control of Hybrid Electric Vehicles Based on Pontryagin's Minimum Principle," *IEEE Trans. Control Syst. Technol.* 19(5):1279-1287, 2011.
34. Onori, S., Serrao, L., and Rizzoni, G., *Hybrid Electric Vehicles Energy Management Strategies* (Springer, 2016).
35. Hegerty, B., Hung, C.-C., and Kasprak, K., "A Comparative Study on Differential Evolution and Genetic Algorithms for some Combinatorial Problems," *Proceedings of 8th Mexican International Conference on Artificial Intelligence*, 2009, 9-13.
36. Storn, R. and Price, K., "Differential Evolution--A Simple and Efficient Heuristic for Global Optimization over Continuous Spaces," *J. Glob. Optim.* 11(4):341-359, 1997.
37. Mamun, A., Narayanan, I., Wang, D., Sivasubramaniam, A. et al., "Multi-Objective Optimization of Demand Response in a Datacenter with Lithium-Ion Battery Storage," *J. Energy Storage* 7:258-269, 2016.
38. T. O. P. TOP, "US Army Test and Evaluation Command Test Operations Procedure," 1995.
39. Kim, Y., Lee, T.K., and Filipi, Z., "Frequency Domain Power Distribution Strategy for Series Hybrid Electric Vehicles," *SAE Int. J. Alt. Power.* 1(1):208-218, 2012, doi:10.4271/2012-01-1003.
40. Liu, Z., Mamun, A., and Onori, S., "Simultaneous Design and Control Optimization of a Series Hybrid Military Truck," SAE Technical Paper 2018-01-1109, 2018, doi:10.4271/2018-01-1109.